Acta Crystallographica Section F
Structural Biology and Crystallization Communications
ISSN 1744-3091

Structural implications of a G170R mutation of alanine:glyoxylate aminotransferase that is associated with peroxisome-to-mitochondrion mistargeting

Snezana Djordjevic,[a] Xiaoxuan Zhang,[b] Mark Bartlam,[c] Sheng Ye,[d] Zihe Rao[c,d] and Christopher J. Danpure[b]*

[a]Structural and Molecular Biology, University College London, Gower Street, London WC1E 6BT, England, [b]Cell and Developmental Biology, University College London, Gower Street, London WC1E 6BT, England, [c]College of Life Sciences, Nankai University, Tianjin 300071, People's Republic of China, and [d]Laboratory of Structural Biology, Tsinghua University, Beijing 100084, People's Republic of China

Correspondence e-mail: c.danpure@ucl.ac.uk

Received 25 September 2009
Accepted 18 December 2009

PDB Reference: G170R-mutant alanine: glyoxylate aminotransferase, 1j04.

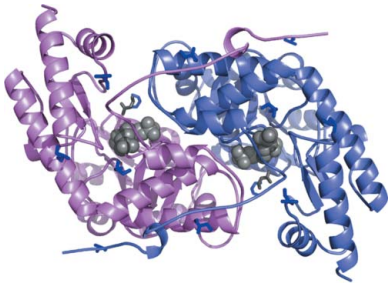

In a subset of patients with the hereditary kidney-stone disease primary hyperoxaluria type 1 (PH1), the liver-specific enzyme alanine:glyoxylate aminotransferase (AGT) is mistargeted from peroxisomes to mitochondria. This is a consequence of the combined presence of the common P11L polymorphism and a disease-specific G170R mutation. In this paper, the crystal structure of mutant human AGT containing the G170R replacement determined at a resolution of 2.6 Å is reported. The crystal structure of AGT consists of an intimate dimer in which an extended N-terminal segment of 21 amino acids from one subunit wraps as an elongated irregular coil around the outside of the crystallographic symmetry-related subunit. In addition to the N-terminal segment, the monomer structure contains a large domain of 261 amino acids and a small C-terminal domain of 110 amino acids. Comparison of the mutant AGT structure and that of wild-type normal AGT shows that the two structures are almost identical, with a backbone-atom r.m.s. deviation of 0.34 Å. However, evidence of significant local structural changes in the vicinity of the G170R mutation might be linked to the apparent decrease in protein stability.

1. Introduction

Primary hyperoxaluria type 1 (PH1; MIM 259900) is an autosomal recessive kidney-stone disease caused by a deficiency of the liver-specific peroxisomal enzyme alanine:glyoxylate aminotransferase (AGT; Danpure, 2001; Danpure & Rumsby, 2004). A wide variety of enzymic phenotypes have been identified in PH1, including a remarkable trafficking defect found in about one third of patients in which ~90% of the AGT is mistargeted from its normal intracellular location in the peroxisomes to the mitochondria (Danpure *et al.*, 1989). Although AGT is still catalytically active after import into the mitochondria, it is metabolically ineffective.

AGT mistargeting is caused by the synergistic interaction between the common P11L polymorphism and a disease-specific G170R mutation (Purdue *et al.*, 1990; Lumb & Danpure, 2000). The polymorphism generates a cryptic mitochondrial targeting sequence (Purdue *et al.*, 1991), while the polymorphism and mutation together inhibit AGT dimerization (Leiper *et al.*, 1996). This explanation for AGT mistargeting highlights an important difference in the conformational requirements of the peroxisomal and mitochondrial protein-import machineries. Whereas peroxisomes can import fully folded oligomeric proteins, mitochondria can only take up unfolded or loosely folded monomeric polypeptides.

The N-terminal extended region of AGT appears to be important in the process of dimerization, which in turn appears to play a significant role in the kinetic partitioning of polymorphic and mutant AGT within the cell (Leiper *et al.*, 1996; Zhang *et al.*, 2003; Lumb *et al.*, 1999). Based on the crystal structure of normal human AGT (PDB entry 1h0c), we have previously suggested that the P11L and G170R replacements might interfere with dimerization by weakening the inter-subunit tethering of the N-terminal extension (Zhang *et al.*, 2003). This could have two effects. Firstly, it would free up the N-terminal polymorphic mitochondrial targeting sequence, allowing it to interact with the mitochondrial import receptor TOM20, and secondly, it would delay the protein from attaining a conformation incompatible with the mitochondrial protein-import machinery (*i.e.* a

Table 1
Data-collection and refinement statistics.

Values in parentheses are for the highest resolution shell.

X-ray data	
Resolution (Å)	50.0–2.60 (2.68–2.60)
R_{merge}	0.092 (0.487)
$\langle I/\sigma(I)\rangle$	11.6 (2.4)
Completeness (%)	97.2 (100)
Unique reflections	18539
Wavelength (Å)	0.9330
Refinement	
R_{work}	0.22 (0.30)
R_{free}	0.27 (0.29)
R.m.s.d. from ideal	
Bond lengths (Å)	0.008
Bond angles (°)	1.50
Dihedral angles (°)	23.0
Improper angles (°)	0.95

fully folded dimer). The importance of protein stability, either of the final dimer or of on-pathway folding intermediates, in the intracellular partitioning of mutant AGT has been demonstrated by the observation that procedures known to increase protein stability nonspecifically, such as lowering the temperature or the addition of chemical chaperones/osmolytes such as glycerol, can completely normalize its targeting in an *in vitro* cell-culture system (Lumb *et al.*, 2003). Not surprisingly, procedures that are known to decrease protein stability, such as increasing the temperature, exacerbate the mistargeting of mutant AGT (Lumb *et al.*, 2003).

In order to gain further insights into the mechanistic basis of AGT mistargeting and how chemical chaperones such as glycerol might correct it, we have solved the X-ray crystal structure of human AGT containing the disease-specific G170R mutation by molecular replacement to a resolution of 2.6 Å. Comparison of the G170R AGT structure with that of the wild-type protein reveals localized changes that might have implications for protein stability and possibly cellular targeting of the enzyme.

2. Experimental procedures

2.1. Protein purification and crystallization

The C-terminally His-tagged construct of mutant (G170R) human AGT in pTrcHis2A, its expression in *Escherichia coli* JM109 and its purification by nickel-resin affinity chromatography have been described previously (Zhang *et al.*, 2001, 2003). Prior to crystallization, the protein was concentrated to a final concentration of 15 mg ml^{-1}. The crystallization of the G170R variant of human AGT in the presence of the cofactor pyridoxal phosphate and the inhibitor aminooxyacetic acid was carried out as described for normal human AGT (Zhang *et al.*, 2001). Prior to diffraction data collection, the crystals obtained from 10% PEG 4000 in 0.1 *M* Na HEPES pH 7.5 buffer were soaked in 20–30% glycerol solution.

2.2. Data collection, structure determination and refinement

Diffraction data were collected at 100 K and recorded using CCD detectors on beamline ID 14-2 at the European Synchrotron Research Facility, Grenoble, France. Diffraction images were integrated using *MOSFLM* (Leslie, 1992) and data were processed using *SCALEPACK* (Otwinowski & Minor, 1997) and *TRUNCATE* (French & Wilson, 1978) from the *CCP*4 program suite (Collaborative Computational Project, Number 4, 1994). All crystals belonged to space group $P4_12_12$, with unit-cell parameters $a = b = 89.49$, $c = 142.82$ Å. The molecular-replacement method was employed using *CNS* (Brünger *et al.*, 1998) with a monomer of a wild-type AGT structure (PDB code 1h0c; Zhang *et al.*, 2003) as a search model. The program *O* (Jones *et al.*, 1991) was used to build the model, while refinement was carried out in *CNS* (Brünger *et al.*, 1998). A total of 113 water molecules and seven glycerol molecules were added in the final rounds of refinement. The atomic coordinates and structure factors have been deposited in the RCSB Protein Data Bank under accession code 1j04. Data-collection and refinement statistics can be found in Table 1. All figures were generated in *PyMOL* (DeLano Scientific LLC, San Carlos, California, USA), which was also used to generate electrostatic potential molecular surfaces.

3. Results and discussion

3.1. Normal and mutant human AGT have a similar overall structural architecture

The X-ray crystal structure of human AGT containing the disease-specific G170R mutation was solved in order to gain further insights into the mechanistic basis of AGT mistargeting. Very much like wild-type AGT (PDB code 1h0c; Zhang *et al.*, 2003), G170R AGT adopts the quaternary structure of an intimate dimer, with a similar loss of solvent-accessible surface area (4038 Å^2) and gain in solvation free energy (−239 kJ mol^{-1}; Lee & Richards, 1971). Each monomer contains an extended N-terminal region of 21 residues that wraps around the surface of another subunit comprising a large N-terminal domain (residues 22–282) and a smaller C-terminal domain (residues 283–392) (Fig. 1). This overall architecture is very similar to that of wild-type human AGT determined at 2.5 Å resolution; the r.m.s. deviation for backbone atoms between the two structures was only 0.34 Å. The N-terminal residues 1–3, C-terminal residues 391–392 and the C-terminal His tag could not be seen in either structure. The residues Ala121 and Arg122 that were missing in the structure of wild-type AGT were visible in the electron density of the G170R-mutant structure. The spatial configurations of the active-site residues, the cofactor pyridoxal phosphate and the competitive inhibitor aminooxyacetic acid in the mutant protein are not significantly different from those in the wild-type protein. This is despite our previous observation that the specific catalytic activity of purified

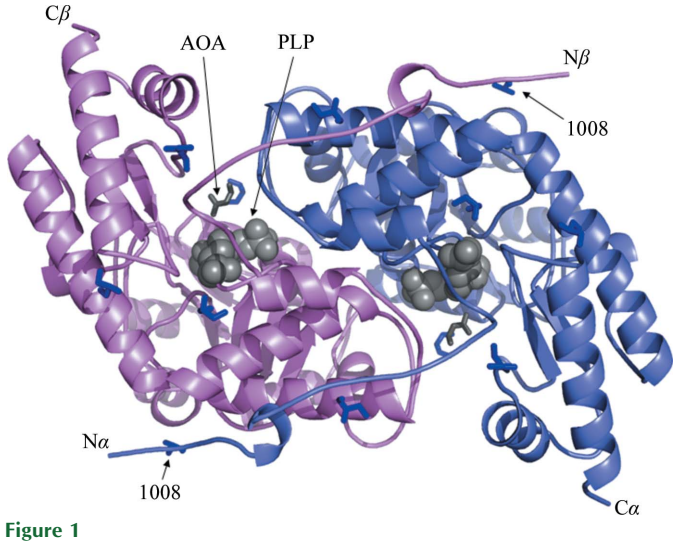

Figure 1
Overall crystal structure topology of G170R AGT. The α-chain is coloured blue and the β-chain is coloured purple. The seven glycerol molecules per subunit resolved in the structure are shown as blue sticks and the aminooxyacetic acid inhibitor is shown as grey sticks. Grey spheres depict the pyridoxal phosphate cofactor in the core of the subunits. Glycerol molecule 1008 near the site of the mutation is labelled.

recombinant G170R AGT is only about 40% of that of the normal protein (Lumb & Danpure, 2000).

3.2. Localized effect of the G170R mutation

The high level of structural similarity between the wild-type protein and the G170R-mutant structure was somewhat surprising as the mutation creates a profound metabolic effect resulting in disease. Gly170 in wild-type AGT is located in the first turn of helix 168–175 and is packed against Gly199 in the loop 184–201 (Fig. 2). In the G170R structure the introduction of the long and positively charged side chain of Arg in place of the H atom of Gly results in significant local conformational changes affecting the backbone of the 168–175 helix. In wild-type AGT Gly170 is positioned very close to Gly199 such that the C^{α} atom of Gly170 is 4.2 Å away from the Gly199 C^{α} atom and 3.5 and 3.4 Å away from the carbonyl O atoms of Gly199 and Gln198, respectively. This close packing arrangement does not allow the introduction of an Arg side chain and as a result of the mutation the 168–175 helix undergoes a conformational change that can be described as an ∼1 Å translation in the position of the C^{α} atom of residue Asp167 preceding the helix combined with an approximately 30° turn along the helical axis (Fig. 2). This helical displacement provides an ∼1.5 Å change in the C^{α} position of residue 170 and roughly a half peptide-bond turn of the helix. Fig. 3 shows details of the conformational changes associated with the introduction of Arg at position 170, while Fig. 4 provides a weighted electron-density map for this area of the crystal structure. Most strikingly, the described rotation of the helix results in the breakage of a salt bridge between His174 and Asp201 in the central β-strand 202–206. The C-terminal end of this strand leads into a helical turn containing the covalently linked PLP cofactor. Introduction of the Arg170 side chain and the rotation of His174 towards solvent additionally impact the molecular surface in the vicinity of the mutation. A clear change in the landscape of the molecular surface is coupled to a reversal in polarity of the surface electrostatic potential from negative in the wild-type protein to positive in G170R AGT (Fig. 5). The described localized changes in the intramolecular interactions and the molecular surface of the G170R-mutant protein could give rise to increased localized unfolding of the polypeptide chain, contributing to the overall decrease in protein stability. However, further biophysical characterization of the G170R AGT variant would be necessary to verify this interpretation.

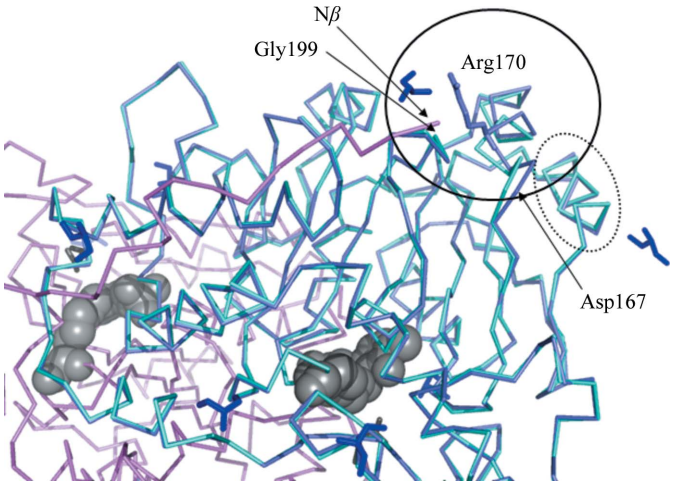

Figure 2
Localized effect of the G170R mutation on the C^{α}-atom representation of AGT. The same colouring scheme is used as in Fig. 1, with additional light-blue C^{α}-atom representation for the α-subunit of the wild-type enzyme. The structures overlap very well, with the exception of helix 168–177 (circled) containing the mutation and a minor impact on the neighbouring helix 134–145 (enclosed within the dotted oval). The side chain of residue Arg170 is shown as a stick model.

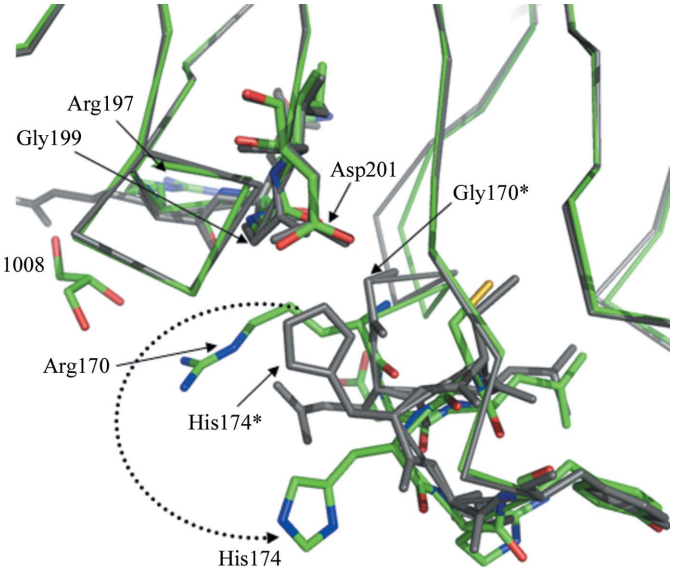

Figure 3
Close-up view of the conformational changes associated with the mutation. The wild-type molecule is coloured grey, while the G170R AGT structure is coloured in an all-atom fashion with green, red, blue and yellow representing C, O, N and S atoms, respectively. For clarity, only those residues that are discussed in the text are shown explicitly. Residues labelled with an asterisk are those of the wild-type AGT structure.

3.3. Glycerol molecules in the G170R AGT structure

Soaking of the crystals in glycerol-containing solution prior to data collection resulted in a number of glycerol molecules being associated with the crystal structure of the G170R AGT protein. The majority of these overlapped closely with the glycerol molecules previously found in the crystal structure of the wild-type protein (Zhang *et al.*, 2003), suggesting that they have bound to the putative glycerol-specific binding sites on the surface of AGT. Glycerol molecule 1008 in the G170R AGT structure occupies one of two newly identified glycerol-binding sites (Figs. 3 and 4). This molecule is within hydrogen-bonding distance of Arg170 and it would be tempting to

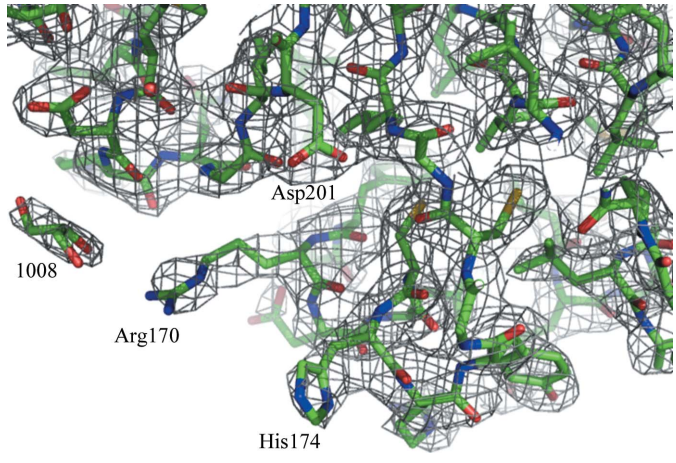

Figure 4
Electron-density map (contoured at the 1σ level) for the region of the structure surrounding the mutation. The map was calculated using the *FFT* routine in *CCP*4 with FWT amplitudes and PHWT phases.

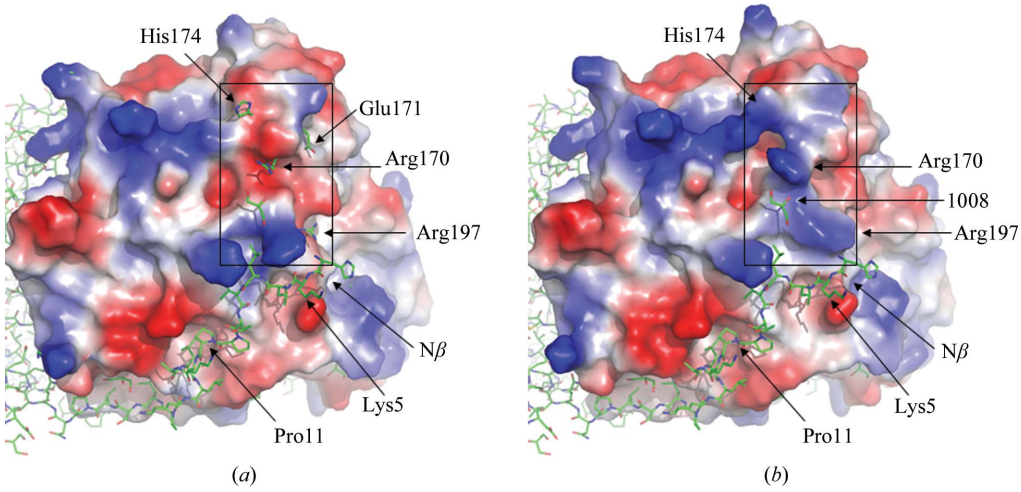

Figure 5
Comparisons of the molecular surfaces of the wild-type and mutant proteins. An all-atom model of the G170R AGT dimer is shown in combination with the molecular surface for the α-subunit coloured based on the surface electrostatic potential. (*a*) The molecular surface of the wild-type protein is overlaid over the all-atom model of the G170R-mutant structure. The side chain of Arg170 is shown as well as the side chains of the residues that have undergone conformational changes and are now protruding from the original wild-type molecular surface. Residue Pro11 that is associated with the disease-related polymorphism is also labelled. (*b*) The molecular surface of the α-subunit of the G170R AGT structure is shown. The surface electrostatic potential in the vicinity of the mutation is now positive compared with the same area of the wild-type molecular surface shown in (*a*). The areas containing the most pronounced changes are emphasized by rectangles drawn around them.

postulate that binding of the glycerol molecule at this site aids in the stabilization of G170R AGT. However, close inspection of the electron density for the wild-type protein crystal structure in this region revealed an unaccounted density of similar size and shape, indicating that a low-occupancy glycerol molecule is probably found in a similar location in the wild-type AGT. This glycerol-binding site is also interesting as it is near to residue Arg197, which has been shown to form a hydrogen bond to the carbonyl O atom of Lys5 from the second subunit of a dimer in the structure of the wild-type protein. Residual electron density in the crystal structure of wild-type AGT (PDB code 1h0c) suggests that an alternative conformation that projects the Arg197 side chain away from this interaction is also present in the structure. Interestingly, in the G170R AGT structure the predominant rotamer of the Arg197 side chain is that which precludes a hydrogen-bond interaction with the carbonyl O atom of Lys5 of the second polypeptide chain within the dimer (Fig. 5). Thus, this change at the interface of the subunits might be an additional source of the aberrant dimer stability.

3.4. Implications for the pharmacological normalization of AGT trafficking as a possible treatment for PH1

There is increasing evidence that in many genetic diseases the primary defect of missense mutations is to disrupt both protein folding and stability. This can lead to protein aggregation, accelerated degradation or aberrant compartmentalization. In this respect, PH1 is a classic genetic disease as mutations are known which result in all of these molecular phenotypes. However, the aberrant compartmentalization of AGT is unique among genetic diseases because it involves not only disruptions to the normal folding and dimerization pathway but also the generation of a cryptic (*i.e.* mitochondrial) targeting sequence (Lumb *et al.*, 1999).

There are a number of known cases in which small-molecule modulators of protein folding and stability, such as chemical chaperones, osmolytes, enzyme inhibitors and receptor antagonists, can counteract the effects of missense mutations on protein function, at least in model systems if not in patients themselves (Lumb *et al.*, 2003; Cohen & Kelly, 2003). Although thermodynamics undoubtedly plays a role in genetic disorders characterized by protein misfolding, it is the kinetics of misfolding and misassembly in the crowded cellular milieu that seems to have a critical influence. Relatively small alterations in the overall rates of folding and dimerization have the potential to normalize aberrant molecular phenotypes and be of benefit to patients with these diseases. The binding of small-molecule nonspecific modulators such as glycerol in the structures of normal and mutant proteins may provide an important clue for the rational design of more specific pharmacological agents.

References

Brünger, A. T., Adams, P. D., Clore, G. M., DeLano, W. L., Gros, P., Grosse-Kunstleve, R. W., Jiang, J.-S., Kuszewski, J., Nilges, M., Pannu, N. S., Read, R. J., Rice, L. M., Simonson, T. & Warren, G. L. (1998). *Acta Cryst.* D**54**, 905–921.

Cohen, F. E. & Kelly, J. W. (2003). *Nature (London)*, **426**, 905–909.

Collaborative Computational Project, Number 4 (1994). *Acta Cryst.* D**50**, 760–763.

Danpure, C. J. (2001). *The Molecular and Metabolic Bases of Inherited Disease*, edited by C. R. Scriver, A. L. Beaudet, W. S. Sly, D. Valle, B. Childs, K. W. Kinzler & B. Vogelstein, pp. 3323–3367. New York: McGraw–Hill.

Danpure, C. J., Cooper, P. J., Wise, P. J. & Jennings, P. R. (1989). *J. Cell Biol.* **108**, 1345–1352.

Danpure, C. J. & Rumsby, G. (2004). *Expert Rev. Mol. Med.* **6**, 1–16.

French, S. & Wilson, K. (1978). *Acta Cryst.* A**34**, 517–525.

Jones, T. A., Zou, J.-Y., Cowan, S. W. & Kjeldgaard, M. (1991). *Acta Cryst.* A**47**, 110–119.

Lee, B. & Richards, F. M. (1971). *J. Mol. Biol.* **55**, 379–400.

Leiper, J. M., Oatey, P. B. & Danpure, C. J. (1996). *J. Cell Biol.* **135**, 939–951.

Leslie, A. G. W. (1992). *Jnt CCP4/ESF–EACBM Newsl. Protein Crystallogr.* **26**.

Lumb, M. J., Birdsey, G. M. & Danpure, C. J. (2003). *Biochem. J.* **374**, 79–87.

Lumb, M. J. & Danpure, C. J. (2000). *J. Biol. Chem.* **275**, 36415–36422.

Lumb, M. J., Drake, A. F. & Danpure, C. J. (1999). *J. Biol. Chem.* **274**, 20587–20596.

Otwinowski, Z. & Minor, W. (1997). *Methods Enzymol.* **276**, 307–326.

Purdue, P. E., Allsop, J., Isaya, G., Rosenberg, L. E. & Danpure, C. J. (1991). *Proc. Natl Acad. Sci. USA*, **88**, 10900–10904.

Purdue, P. E., Takada, Y. & Danpure, C. J. (1990). *J. Cell Biol.* **111**, 2341–2351.

Zhang, X., Roe, S. M., Hou, Y., Bartlam, M., Rao, Z., Pearl, L. H. & Danpure, C. J. (2003). *J. Mol. Biol.* **331**, 643–652.

Zhang, X., Roe, S. M., Pearl, L. H. & Danpure, C. J. (2001). *Acta Cryst.* D**57**, 1936–1937.